New Evidence for a Membrane-Bound Pathway in Hormone Receptor Binding†

Luis Moroder,*,‡ Roberta Romano,‡ Wolfgang Guba,§ Dale F. Mierke,§ Horst Kessler,§ Christine Delporte,∥ Jacques Winand,∥ and Jean Christophe∥

Max-Planck-Institute für Biochemie, D-82143 Martinsried, Germany, Organisch-Chemisches Institut, TU München, München, Germany, and Laboratoire de Chimie Biologique et de la Nutrition, Université Libre de Bruxelles, Bruxelles, Belgium

Received August 13, 1993; Revised Manuscript Received September 27, 1993®

ABSTRACT: The fully active cholecystokinin analog (Thr,Nle)-CCK-9 was lipo-derivatized by N-terminal grafting of a dimyristoylglycerol moiety to induce tight interdigitation with cell membrane bilayers. While the parent CCK peptide was shown to interact only transiently with small unilamellar phospholipid vesicles, the lipo-CCK peptide, although self-aggregating into vesicles, inserts rapidly and quantitatively into phospholipid bilayers. Fluorescence and, even more so, NMR data are supportive for a chain reversal of the CCK moiety of the lipo derivative with embedment of the C-terminus into hydrophobic compartments of the bilayer. MD simulations allowed for a proposal of the folded form of CCK in bilayers with a helical array parallel to the interface and an amphipathic display of the side chains. In this model, the phenylalanine aromatic ring is heading the peptide molecule and may thus play a decisive role in the lateral penetration of the receptor at the water/lipid interface. In fact, despite the membrane-bound state, its binding affinity for rat pancreatic acini is comparable to that of the CCK peptide when tested after a 3-h equilibration period but 5–6-fold lower at 45 min, suggesting that the association rate is significantly lower than that of the unmodified CCK peptide. This can rationally be attributed to the tight interdigitation of the double-tailed lipo moiety with the membrane bilayer. Moreover, an escape of the lipopeptide into the extracellular aqueous phase is energetically highly unfavored; therefore, the receptor can only be reached by a membrane-bound two-dimensional migration. The observed difference in amplification between binding and amylase secretion may result from inadequate occupation of low-affinity CCK receptors, which leads then to poor couplings to G-proteins. Nevertheless the data confirm that lateral penetration of receptor structures is possible, and thus, preadsorption of peptide (neuro)hormones at the cell membrane bilayer may indeed represent the first step in the receptor recognition process.

The cholecystokinin (CCK)[1]/gastrin family of peptides was originally isolated from the pig gastrointestinal tract (Tracy & Gregory, 1964; Mutt & Jorpes, 1968). Since then, it has been found in the central nervous system, where the predominant form corresponds to the cholecystokinin octapeptide (CCK-8) in the sulfated and unsulfated forms (Dockray, 1978; Robberecht et al., 1978; Rehfeld et al., 1985). The CCK/gastrin peptides are known to exert their physiological function via two receptor subtypes of well-defined structure (Wank et al., 1992a,b; Kopin et al., 1992), i.e. the CCK_A receptor, mainly located in the pancreas and selective for the sulfated forms of CCK peptides, and the CCK_B receptor, widely distributed in the central nervous system and in the gastrointestinal tract, which recognizes CCK and gastrin peptides with similar affinities independently of their state of sulfation.

A comparison of the sequences of the CCK_A and CCK_B receptors shows 48% identity as expected for receptors within the same family (Wank et al., 1992a). From a hydropathy plot of the sequences and in analogy to other members of the G-protein-coupled receptor superfamily, seven putative transmembrane domains were identified which are connected by extra- and intracellular loop domains. Cysteines in the first and second extracellular domains are conserved in both receptors and may be involved in disulfide bridges as required for the stabilization of these domains, similar to what was found in rhodopsin, β-adrenergic, and muscarininc receptors (Karnik et al., 1988; Dixon et al., 1987; Hulme et al., 1990). Moreover, three potential asparagine-linked glycosylation sites are identified in the N-terminal domain which account for the higher M_r values deduced from affinity labeling of the receptors (Sakamoto et al., 1984).

The structure of the superfamily of receptors containing seven transmembrane domains is believed to consist of a bundle of helices spanning the cellular membrane with the variously large connecting loops forming bulky functional domains exposed to the extra- and intracellular aqueous phases (Savarese & Fraser, 1992).

Recognition of peptide hormones by such membrane-bound receptors can either occur directly from the extracellular aqueous phase via collision with surface-exposed binding sites or be mediated by the statistically more favored preadsorption on the target cell membrane. Besides reducing the dimensionality of the collisional process for hormone receptor binding, accumulation of the peptides on the lipid bilayer has been proposed to induce orientations and conformations which meet more properly the structural and stereochemical re-

† This study was partly supported by Grant SC1/CT91-0632 from the Commission of the European Communities and by Grant SFB 266 from the Deutsche Forschungsgemeinschaft.

* To whom correspondence should be addressed.
‡ Max-Planck-Institut für Biochemie.
§ TU München.
∥ Université Libre de Bruxelles.

® Abstract published in *Advance ACS Abstracts*, November 15, 1993.

[1] Abbreviations: CCK, cholecystokinin; HG-17, human little gastrin; (Thr,Nle)-CCK-9, (Thr^{28},Nle^{31})-CCK-(25–33); [^{125}I]-(Thr,Nle)-CCK-9, radioiodinated desaminotyrosyl-(Thr,Nle)-CCK-9; DM-CCK, (2*R*,*S*)-1,2-dimyristoyl-3-mercaptoglycerol/N^{α}-maleoyl-β-alanyl-(Thr,Nle)-CCK-9 adduct; DMPC, dimyristoylphosphatidylcholine; hs-DSC, high sensitivity differential scanning calorimetry; CD, circular dichroism; SUV, small unilamellar vesicle; NOESY, nuclear Overhauser effect spectroscopy; TOCSY, total correlation spectroscopy; COSY, correlation spectroscopy; MD, molecular dynamics; IP_3, inositol 1,4,5-triphosphate; G-protein, guanine nucleotide binding protein.

0006-2960/93/0432-13551$04.00/0

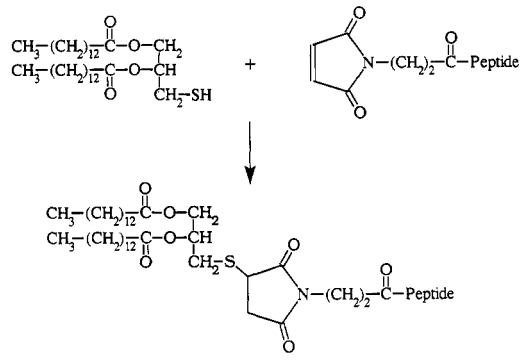

Peptide: Arg-Asp-Tyr(SO_3)-Thr-Gly-Trp-Nle-Asp-Phe-NH_2 [Thr^{28},Nle^{31}]-CCK-(25-33)

FIGURE 1: Chemical structure of the lipophilic CCK peptide (DM-CCK).

quirements of the receptor than the random structure usually adopted by unrestrained peptides in the extracellular aqueous phase (Schwyzer, 1986, 1991). This, however, would imply a membrane-bound two-dimensional migration of the peptides to the receptor binding site and, thus, a lateral penetration of the complex channel-type receptor structure at the water/lipid boundary. A verification of this hypothetical mechanism could possibly be derived by drastically shifting the partition equilibrium of regulatory peptides between the aqueous extracellular phase and the membrane bilayer in favor of the lipid phase. For this purpose lipophilic derivatizations represent a promising approach, particularly if double-tailed lipo moieties are used as anchors to guarantee tight interdigitation with lipid bilayers.

We have previously developed thiol-functionalized bis(fatty acyl)glycerols to be used in thiol–maleimide reactions for selective lipo modifications of peptides (Moroder et al., 1990). Using this procedure 1,2-dimyristoyl-3-mercaptoglycerol was linked covalently to the N^{α}-maleoyl-β-alanyl derivative of (Thr,Nle)-CCK-9, a fully active CCK analogue (Moroder et al., 1981), to produce the lipophilic CCK adduct (DM-CCK) (Romano et al., 1993b) shown in Figure 1. Since N-terminal derivatization of CCK peptides is not expected to affect significantly their bioactivity profile (Winand et al., 1991a; Moroder et al., 1993a), the lipo-CCK derivative *a priori* should largely retain its hormonal properties. The lipid-type structure was found to induce self-aggregation of the lipo-CCK derivative on vortexing in aqueous solution with formation of a polydispersed system of unilamellar vesicles. The high degree of fluidity of these vesicles, however, allows for a fast and net transfer of DM-CCK to small unilamellar vesicles of dimyristoylphosphatidylcholine (DMPC SUV) even below the phase-transition temperature of the DMPC bilayer whereby CCK-rich domains are formed, as well assessed by microcalorimetric experiments (Romano et al., 1993a). Thus, a merging of DM-CCK vesicles with cell membranes should occur likewise easily and quantitatively.

In the present study, the lipo-CCK derivative and the parent (Thr,Nle)-CCK-9 analogue were compared in their receptor-binding affinities and amylase secretion potencies using isolated rate pancreatic acini, which are known to contain the CCK_A subtype receptor. Moreover, the location, orientation, and conformation of the lipopeptide at the lipid/water interface were assessed by spectroscopic measurements combined with molecular dynamics (MD) simulations. A correlation of the biological properties with the conformational state has allowed for definition of a potential two-dimensional migration of the membrane-bound CCK peptide to the receptor, a fact which can only be explained rationally if sufficient mobility of the complex transmembrane structure allows for lateral penetration at the lipid/water interface.

EXPERIMENTAL PROCEDURES

Materials

The synthesis and analytical characterization of the peptides used in the present study were described elsewhere: (Nle^{15})-HG-17 (Moroder et al., 1983), (Thr,Nle)-CCK-9 (Moroder et al., 1981), DM-CCK (Romano et al., 1993a). DMPC and DPPC were from Fluka AG (Buchs, Switzerland).

Methods

Sample Preparation. Peptide concentrations were determined by weight and peptide content and further controlled by UV absorption measurements. All buffers were filtered through a 0.2-μm polycarbonate filter (Millipore). Aqueous solutions of (Thr,Nle)-CCK-9 and (Nle^{15})-HG-17 were prepared by dissolving the peptide samples in 0.1% ammonia (5% of the final volume) and diluting with 5 mM phosphate buffer containing 100 mM NaCl (pH 7.0). Stock solutions of DM-CCK were prepared by taking up weighed samples in 5% ammonia (5% of the final volume), diluting with the above buffer, and vortexing at 30 °C until clearance. Phospholipid SUVs were prepared by suspending weighed samples of the lipid in 5 mM phosphate buffer containing 100 mM NaCl (pH 7.0) and sonicating with a Branson titanium rod sonifier in a cooling bath for short periods of time until optically transparent vesicle preparations were obtained. These were incubated at 30 °C for 1 h and then centrifuged in order to remove titanium dust contamination from the sonifier rod.

High-Sensitivity Differential Scanning Calorimetry (hs-DSC). hs-DSC measurements were performed with a MC-2 microcalorimeter (Microcal, Amherst, MA) at a scan rate of 45 °C/h (ascending temperature mode only) interfaced to an IBM AT microcomputer. The data were stored and analyzed using the DA-2 software provided by Microcal. Stock solutions of peptides in phosphate-buffered saline (pH 7.0) were added to the phospholipid SUV preparations to reach final peptide concentrations in the range 2.4×10^{-4} to 3×10^{-4} M and peptide:lipid molar ratios of 1:12.

Circular Dichroism (CD). CD spectra were recorded on a Jobin-Yvon dichrograph Mark IV equipped with a thermostated cell holder and connected to a data station for signal averaging and processing. All CD measurements were performed at 20 °C, and the data averages were of 10 scans. The peptides were incubated at 3.2×10^{-5} M concentrations with sonicated DMPC and DPPC vesicle preparations for 2 h at 50 °C prior to the measurements. Quartz cells with 0.1-cm optical paths were used.

Nuclear Magnetic Resonance (NMR). A 2 mM sample for NMR analysis was prepared by taking up the weighed amount of DM-CCK (95% peptide content as determined by quantitative amino acid analysis) (Romano et al., 1993a) in 25 μL of 0.1% ammonia and diluting with 5 mM phosphate buffer containing 100 mM NaCl and 10% ^2H_2O in the final volume; the pH was adjusted to 5.4 (uncorrected for isotope effects). At the pH and ion strength chosen for the NMR experiments, the vesicle preparations were found to be sufficiently stable for longer periods of time, as required for the measurements. The NMR spectra were recorded at 37 °C on a Bruker AMX-600 spectrometer, operating at 600 MHz. Data were processed on Bruker X32 work stations using the UXNMR program.

The spectra of nuclear Overhauser effect spectroscopy (NOESY) were recorded with 400–512 increments in the t_1 dimension, 64–126 scans, mixing times of 20, 50, 100, and 150 ms, a relaxation delay of 1.3 s, and 4K data points in t_2. A 1–1 (jump–return) observation pulse (Plateau & Gueron, 1982), with a delay of 85 μs, was used. In addition, the mixing pulse was phase-shifted by 45° to reduce radiation damping (Driscoll et al., 1989). Pure absorption spectra were obtained using the TPPI method (Bodenhausen et al., 1980; Marion & Wüthrich, 1983). The data set was zero-filled to produce a matrix of 4K × 2K and a shifted sine bell function applied prior to Fourier transformation.

The spectra of total correlated spectroscopy (TOCSY) were recorded with 96–128 scans, a relaxation delay of 1.2 s, 320–512 t_1 increments, and 2K data points in t_2. Various mixing schemes were used for the spin-locking period, including MLEV-17 (with and without trim pulses), MLEV-16, and DIPSI-2 all with a 10-kHz spin-locking field strength. A 90° flip back pulse to align the magnetization along the z axis followed by a 4-ms homospoil pulse and a 4-ms recovery delay (Sklenar & Bax, 1987; Bax et al., 1987) was used before a 1–1 observation pulse (Plateau & Gueron, 1982) with a delay of 85 μs. Additional spectra using presaturation during the relaxation delay were acquired with and without the 1–1 observation pulse. Prior to Fourier transformation, the time domain data were zero-filled to a final data matrix of 4K × 2K multiplied by a shifted sine bell function.

A spectrum of PE correlation spectroscopy (COSY) (Müller, 1987) was recorded with 8192 data points in t_2, 64 scans, 600–880 points in t_1, and relaxation delay of 1.2 s. The reference one-dimensional proton spectrum was recorded with 16 384 points. The relaxation delay was equal to the relaxation delay of the two-dimensional experiment reduced by the acquisition time of the experiment, and delay before acquisition was equal to $2\tau_p/\pi + 2$ μs, where τ_p is the length of a 37′ proton pulse. The reference spectrum was subtracted from the two-dimensional spectrum before Fourier transformation. Data were twice zero-filled and apodized with a squared sine bell function shifted by $\pi/3$ in both dimensions.

Computational Procedures. Molecular dynamics (MD) simulations and interactive modeling were performed with DISCOVER (consistent valence force field without morse potential or cross terms) and INSIGHT II from Biosym Technologies (San Diego, CA) on Silicon Graphics Crimson and 4D/240 SX computers. The starting structure of DM-CCK was built up by taking into account the preferred conformation of (Thr,Nle)-CCK-9 in the cryomixture dimethyl sulfoxide/water (Moroder et al., 1993b), i.e. with a salt bridge between the guanido side-chain function of arginine-1 and the *O*-sulfate hemiester of tyrosine-3 and a γ-turn centered at threonine-4 followed by a 3_{10}-helix up to the C-terminus. For modeling of the lipomoiety and spacer the (2*R*,3′*S*)-diastereomer was chosen arbitrarily, as the configuration at the two carbons was not expected to affect the folding of the peptide portion. All ionizable groups were treated as charged species without inclusion of counterions. Artificial distance restraints between carbonyl oxygens (i = 3–6) and amide hydrogen atoms (i + 3) were used to maintain the secondary structure elements. Additional distance restraints between the indole nitrogen and C6/C7 of either fatty acid chain were applied during the *in vacuo* minimization to force tryptophan-6 into a hydrophobic environment as determined by fluorescence measurements (Romano et al., 1993a) and NMR spectroscopy (present study) of DM-CCK. The fatty acid chains and the glycerol portion were fixed. The system was minimized using a conjugate gradients algorithm until a convergence criterion of 0.01 kcal/Å was reached.

The molecule was then placed in a two-phase (H_2O/CCl_4) simulation cell employing three-dimensional periodic boundary conditions. The details of this simulation cell will be described elsewhere (W. Guba and H. Kessler, unpublished results). DM-CCK, with its fatty acids orthogonal to the phase interface, was soaked up to the ester groups of the glycerol moiety with CCl_4; the rest, with water. The Lennard-Jones parameters for H_2O and CCl_4 and the charges for H_2O were taken from Berendsen et al. (1981) and Rebertus et al. (1979), respectively. The geometric mean was used for the parameters between unlike atoms. The final system consisted of 128 CCl_4 and 609 water molecules with a box size of $x = z = 35$ Å and $y = 43$ Å. Compared to those for an explicit membrane model, the requirements of CPU time are of orders of magnitude less. For the subsequent MD simulations, a time step of 1 fs was employed. Neighbor lists for calculation of nonbonded interactions were updated every 10 steps within a radius of 13 Å. The actual calculation of nonbonded interactions was carried out up to a radius of 11 Å. No switching function was applied. Except for CCl_4 (united-atom model for C), all atoms were treated explicitly. The same constraints as in the *in vacuo* simulation except for the distance restraints between the tryptophan-6 side chain and the fatty acid chains were applied with a maximum force of 1000 kcal·mol^{-1}·Å^{-1}. All atoms were allowed to move freely. After minimization until a convergence criterion of 1.0 kcal/Å, the system was gradually heated in cycles of 1 ps from 10, 50, 100, 250 up to 310 K. The pressure was maintained at 1.0 bar. Equilibration was allowed for another 162 ps. After this, the force constant of the distance restraints was scaled by 0.1, and the following production run of 150 ps with sampling of structures every 200 fs was used for analysis.

Biological Assays. Rat pancreatic acini (3.2 mg), isolated as described previously (Dehaye et al., 1986), were incubated with the CCK peptides at 37 °C for 30 min in 0.2 mL of standard incubation medium consisting of 24.5 mM Hepes buffer (pH 7.4) with 98 mM NaCl, 6 mM KCl, 2.5 mM NaH_2PO_4, 1 mM $MgCl_2$, 0.5 mM $CaCl_2$, 11.5 mM glucose, 5 mM sodium fumarate, 5 mM sodium pyruvate, 5 mM sodium glutamate, 2 mM glutamine, 1% (w/v) amino acid mixture BME witho ut glutamine (Gibco Europe, Uxbridge, Middlesex, U.K.), 1% (w/v) bovine serum albumin, and 500 kallikrein inhibitor units/aprotinin (Trasylol, Bayer). Amylase release was measured with appropriate controls as described (Dehaye et al., 1986), and inositol 1,4,5-triphosphate (IP_3) was determined after a 10-min incubation as previously reported (Winand et al., 1991a).

Binding of CCK peptides to the CCK receptor on rat pancreatic acini was measured using 4.9 nM radioiodinated 3-(4-hydroxyphenyl)propionyl-(Thr,Nle)-CCK-9 (Svoboda et al., 1984) as tracer. Binding experiments were performed by incubation in the same medium as above, enriched with 1 mg/mL bacitracin at 37 °C for 45 min and 3 h as reported previously (Winand et al., 1991a).

For the biological assays stock solutions of (Thr,Nle)-CCK-9 and DM-CCK were prepared as described above for the spectroscopic measurements.

RESULTS

Interaction of CCK Peptides with Lipid Bilayers. The CD spectra of CCK peptides of increasing chain length in aqueous solution are characterized by extremely weak intensities and anomalously low signal to noise ratios, whereas in aqueous

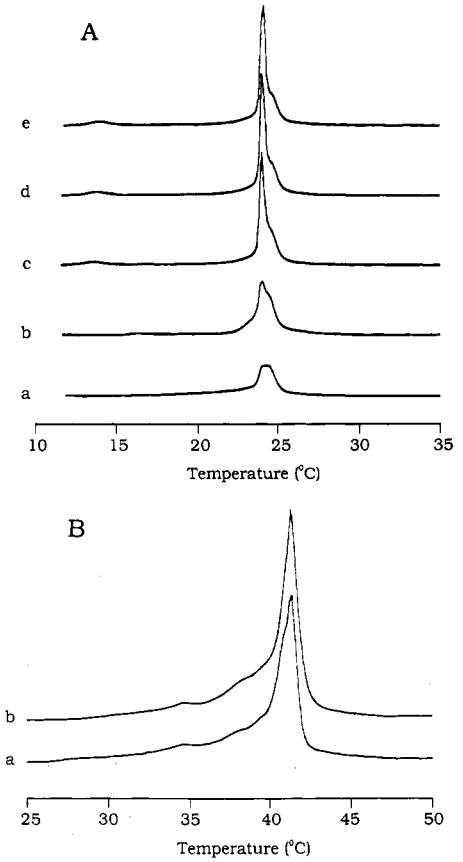

FIGURE 2: hs-DSC endotherms of a 1:12 (molar) mixture of (Thr,Nle)-CCK-9 and (Nle[15])-HG-17 and phospholipid SUVs at scan rates of 45°/h. Panel A shows changes in time of the endotherm of DMPC SUVs in the presence of (Thr,Nle)-CCK-9: (a) scan of DMPC vesicles in absence of peptide as resulting from sonication; (b) first scan of the DMPC/peptide mixture; (c) fourth scan; (d) seventh scan; (e) tenth scan. Further scanning was not found to produce additional changes, and the pattern of the endotherm indicates a mixture of middle-size pure unilamellar DMPC vesicles and SUVs still interacting with the CCK peptide. Panel B shows changes in time of the hs-DSC endotherms of DPPC SUVs in the presence of (Nle[15])-HG-17: (a) endotherm of DPPC vesicles in absence of peptide (the pattern of the endotherm reflects a polydispersed system of unilamellar vesicles); (b) ninth scan of the DPPC/peptide mixture.

trifluoroethanol α-helix-like spectra were obtained although of relatively low intensities (Moroder et al., 1993). Conversely, the dichroic properties of (Thr,Nle)-CCK-9 were not found to change significantly upon its addition to increasing amounts of DMPC and DPPC vesicle preparations at lipid:peptide molar ratios of $\leq$100 (data not shown), but a marked increase in turbidity of the solutions was observed. In this context, it is worth noting that with (Nle[15])-HG-17 an increased turbidity could not be observed and the CD spectra in the presence of DPPC or DMPC were similar to those of the peptide in water and thus characteristic of random-coil structures. The intensity of the negative maximum at 198 nm was decreased and slightly red-shifted to 200 nm. By these spectroscopic techniques it could not be shown that the two homologous peptides are interacting with the lipid bilayer.

In microcalorimetric experiments incubation of (Thr,Nle)-CCK-9 with DMPC SUVs led in a first step to a sharpening of the DMPC endotherm with formation of a shoulder corresponding to about 50% of the total peak area as shown in Figure 2A. Concomitantly, the pretransition temperature appears at higher values in comparison to that of pure DMPC and the observed changes are consistent with an interaction of the CCK peptide with the bilayer. In subsequent scans, the intensity of the shoulder decreased, the main peak became

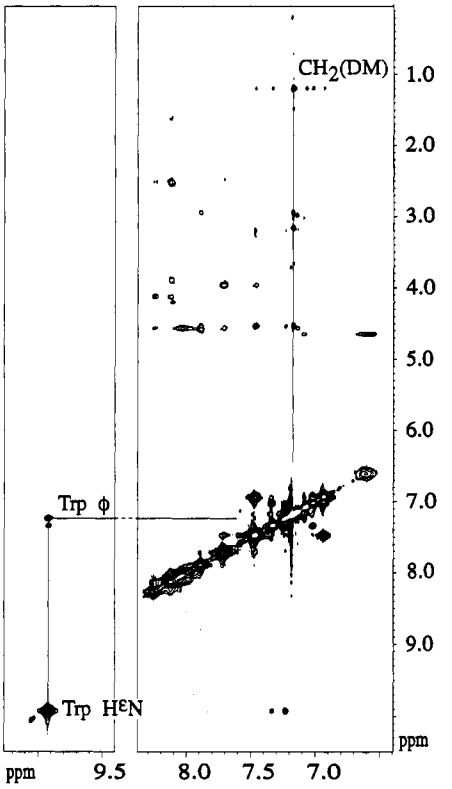

FIGURE 3: Close proximity of the tryptophan side chain and DMPC bilayer illustrated in an expanded portion of a NOESY spectrum (mixing time 50 ms). NOEs between the HN of the indole ring of tryptophan and the aromatic protons and then the alkane chain of the dimyristoyl moieties are highlighted.

sharper, and the pretransition temperature shifted to lower values. These effects suggest that in a second step the CCK peptide is expelled from the bilayer of the vesicles which have fused to larger ones, resulting in a sharp peak with a phase-transition temperature at 24 °C and a pretransition temperature at 14 °C, similar to the case of pure DMPC vesicles. Thus, (Thr,Nle)-CCK-9 inserts into SUVs, causes fusion, and is then expelled because of the higher degree of order of the bilayer packing in large vesicles. These findings agree with the enhanced turbidity observed in the CD experiments. By contrast, addition of (Nle[15])-HG-17 to DPPC SUVs provokes only negligible changes of the endotherm, thus excluding an interaction of this peptide with the bilayer as shown in Figure 2B.

Conformational Properties of DM-CCK. In our previous study, the dichroic properties of the peptide moiety of DM-CCK were found to be practically identical in the DM-CCK vesicles and after their net transfer to DMPC SUVs, a fact which was attributed to the formation of DM-CCK domains (Romano et al., 1993a). Because of the opposite contributions of the aromatic chromophores to the dichrosim of this relatively short peptide, an unambiguous interpretation of the CD spectra was not possible. Nevertheless, the spectra were strongly supportive for β-type structures. The results led us to conclude that the conformations of the CCK peptide are very similar in both environments. Correspondingly, NMR measurements performed on DM-CCK SUVs were expected to yield useful information on the conformational state of DM-CCK also when inserted into artificial membranes. In the NMR experiments, magnetization transfer through bonds via COSY and TOCSY could not be observed because of extremely broad resonances, and therefore a complete resonance assignment was not possible. However, the characteristic spin pattern of the tryptophan-6 residue allowed for an unambiguous as-

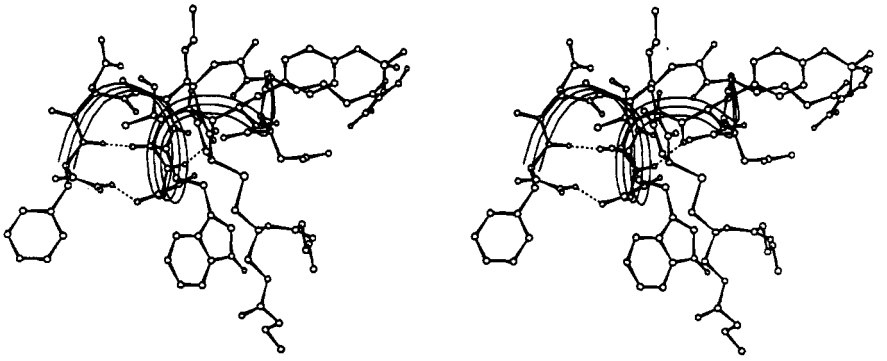

FIGURE 4: Stereoview of the averaged and energy-minimized conformation of DM-CCK. Apolar hydrogens and the major part of the myristoyl moieties have been omitted for clarity. Hydrogen bonds have been indicated by dashed lines, and the helical portion has been illustrated by a ribbon.

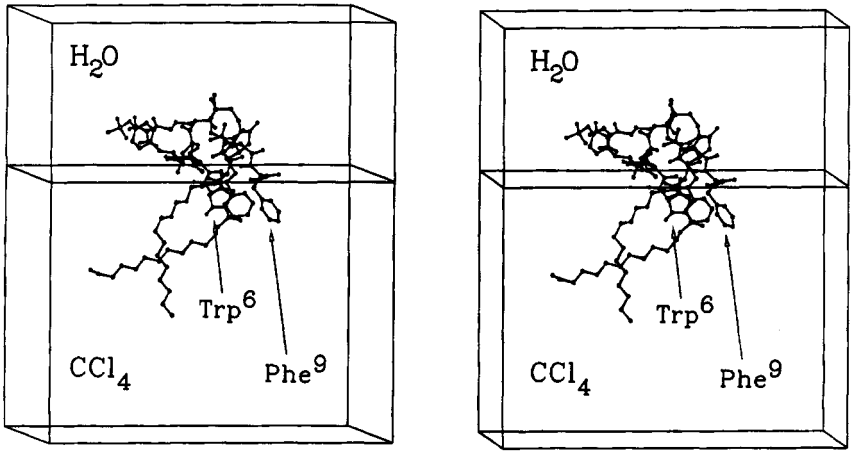

FIGURE 5: Stereoview of the averaged and energy-minimized conformation of DM-CCK superimposed on the averaged position in the biphasic H_2O/CCl_4 cell. Apolar hydrogens of the solute and the solvent molecules have been omitted for clarity. The phase interface has been chosen as the intersection of the H_2O- and CCl_4-density profiles.

signment of an NOE between the indole group of the peptide moiety and the myristoyl alkane chain of the lipid portion as shown in Figure 3. Similar NOEs have been reported for SDS micelles and aromatic residues of small peptides (Hicks et al., 1988). Moreover, a certain degree of conformational order could also be deduced from the NOESY spectrum, although without proton assignments the type and the location of the ordered conformation could not be identified. Embedment of the tryptophan residue into inner compartments of the bilayer was postulated from fluorescence-quenching experiments (Romano et al., 1993b).

Averaged Conformation and Orientation of DM-CCK at the Interface of a Water/CCl_4 System. An insertion of the C-terminus of the CCK moiety into inner compartments of the lipid phase would require a chain reversal with exposure of the charged peptide portion, i.e. Arg-Asp-Tyr(SO_3H), to the water phase. On the basis of this working assumption, a starting structure of DM-CCK for MD simulations was built up with a peptide backbone folding adapted to the preferred conformation of (Thr,Nle)-CCK-9 in the cryomixture dimethyl sulfoxide/water (Moroder et al., 1993b) and with the tryptophan-6 in close contact with the fatty acid chains as suggested above by NMR experiments. The MD simulation was performed in a CCl_4/H_2O cell, which mimics the liquid-crystalline L_a phase of a phospholipid membrane with water representing the polar head groups and the neighboring water phase and CCl_4 representing the unordered lipophilic chain matrix.

The conformation of DM-CCK was averaged and energy-minimized *in vacuo* until a convergence criterion of 0.1 kcal/Å. As can be seen in Figure 4, the γ-turn at threonine-4 is maintained and the C-terminus adopts a helical conformation with a superimposed β-sheet hydrogen-bonding pattern between the threonine-4 carbonyl and phenylalanine-9 amide and between the glycine-5 carbonyl and a C-terminal amide hydrogen atom (populations of about 80 and 70%, respectively). Additional hydrogen bonds are formed between the tyrosine-3 carbonyl and glycine-5 amide (population of 90%) and between the threonine-4 carbonyl and aspartic acid-8 amide (population of about 20%). The latter hydrogen bond has also been observed in the solution structure of (Thr,Nle)-CCK-9, stabilizing the conformation via formation of a 13-membered ring (Moroder et al., 1993b). In Figure 5 the averaged and minimized structure of DM-CCK illustrates its orientation in the simulation cell. The phase interface has been schematically depicted from the density profile as described below. The helix axis of the C-terminal portion lies parallel to the interface, separating hydrophobic from hydrophilic residues, the only exception being norleucine-7, which points into the water phase. Tryptophan-6 is buried in the hydrophobic phase shielded by phenylalanine-9. This hydrophobic clustering compares well with the observed strong blue shift of the fluorescence emission maximum and with the reduced Stern–Vollmer iodide-quenching constant (Romano et al., 1993a). It also agrees with the observed NOE in the NMR measurements. The fatty acid chains move freely in the simulation cell, as there are no restraints to maintain the orientation that would be found within a membrane.

Density Profiles and Radial Distribution Functions of DM-CCK at the Interface. To demonstrate the partition behavior between the two phases, the probability distribution and the time course of the y coordinate (long cell axis) of selected

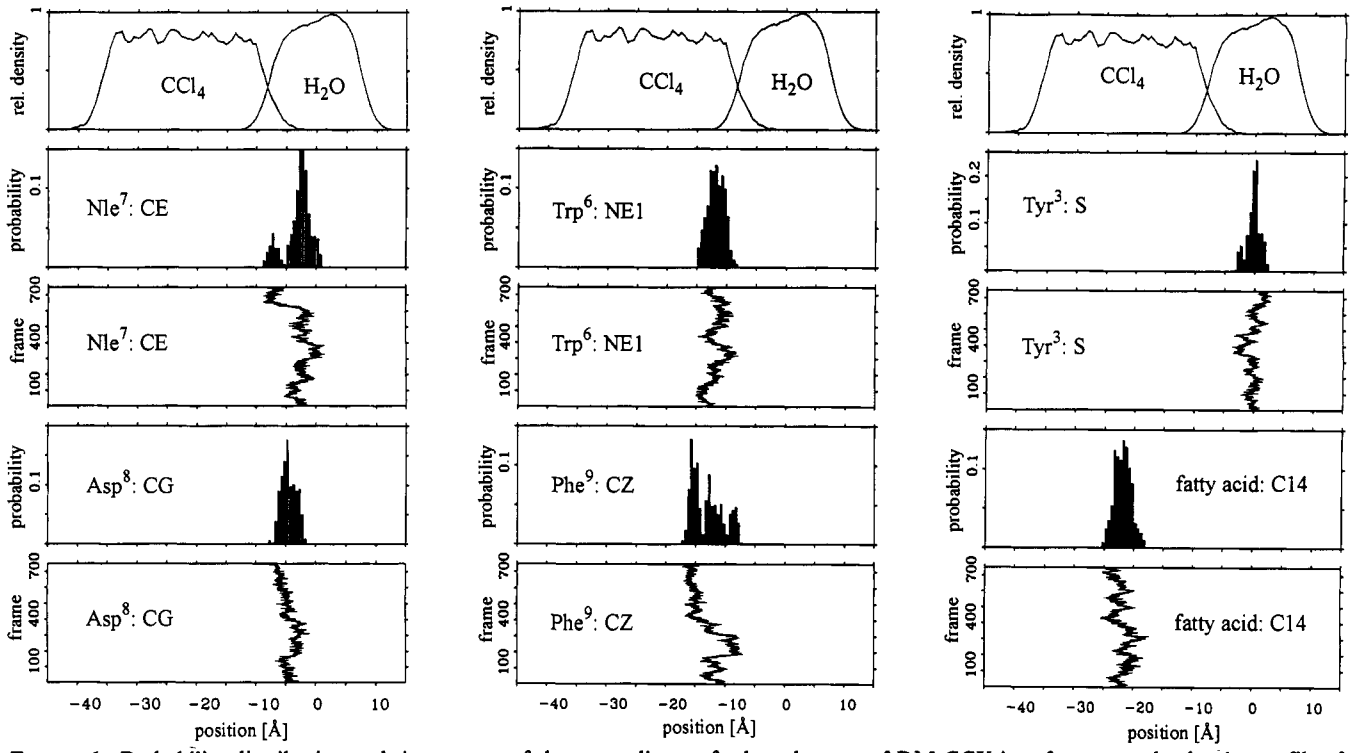

FIGURE 6: Probability distribution and time course of the y coordinate of selected atoms of DM-CCK in reference to the density profile of CCl_4/H_2O.

atoms relative to the density profile were calculated. The atomic density profiles are defined as the average number of oxygen atoms (for H_2O) and carbon atoms (for CCl_4) in cross sections of thickness $\Delta y = 0.5$ Å, normalized to the number densities of liquid water and CCl_4. The origin of the density profile is defined as the arithmetic center of the water molecules averaged over the trajectory. For illustration purposes the phase interface in Figure 5 has been defined as the intersection between the H_2O- and CCl_4-density profiles. The time course of selected atoms in the y direction relative to the coordinate system of the density profiles has been depicted for single atoms in Figure 6. As can be seen, the side chains of norleucine-7 and aspartic acid-8 are mainly exposed to the water phase close to the interface (left panel), whereas phenylalanine-9 and tryptophan-6 are shielded by hydrophobic clustering (center panel). For a comparison, the corresponding plots for one of the fatty acid chain termini and the sulfur atom of the sulfated tyrosine-3 side chain are included to demonstrate the phase partition behavior of groups with greatly differing polarities (right panel).

The formation of solvation shells can be characterized by radial distribution functions (rdfs), $g_{xy}(r)$, which give the probability of finding an atom type y at a distance r from the atom of type x. The rdfs of the sulfur atom of tyrosine-3 and CG of aspartic acid-8 as well as of HZ of phenylalanine-9 and the hydrogen atom of the tryptophan-6 side chain relative to water oxygens were calculated. The rdfs were normalized by dividing the number of water oxygens by the bulk number densities. The rdfs in Figure 7 complement the conclusions from the probability distribution relative to the density profiles mentioned above. Both charged side chains are strongly solvated, whereas phenylalanine-9 and especially tryptophan-6 are buried in a hydrophobic environment without formation of solvation shells.

Biological Properties of DM-CCK. Pancreatic acini were incubated with radioiodinated desaminotyrosyl-(Thr,Nle)-CCK-9 in the presence of either (Thr,Nle)-CCK-9 or DM-

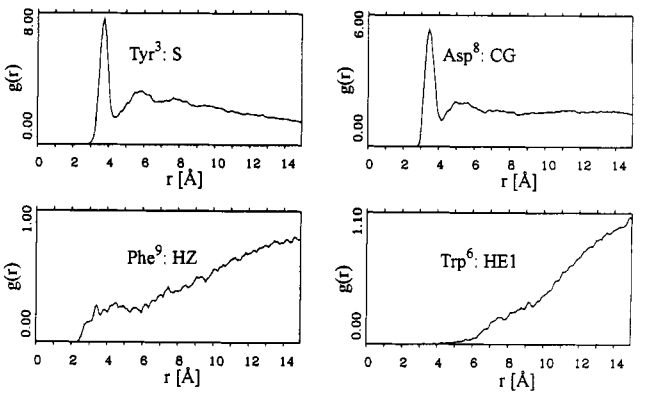

FIGURE 7: Radial distribution functions of selected atoms with water oxygens.

CCK for 45 min and 3 h. The resulting competitive binding curves are shown in Figure 8. After 45-min incubation, the lipo-CCK derivative exhibited an apparent IC_{50} 5–6-fold higher than that of the parent analog (Figure 8a). Extending the incubation to 3 h to allow binding equilibrium of the lipo derivative decreased the IC_{50} of lipo-CCK (Figure 8b). This suggested that the lipophilic derivative had a significantly lower association rate. Analysis of the data in Figure 8b with the nonlinear, least-squares curve-fitting LIGAND program, after Cheng and Prusoff (1973) correction, confirmed that, at binding equilibrium, both high- and low-affinity receptors were occupied by the two peptides (Sankaran et al., 1980; Wank et al., 1988; Menozzi et al., 1991; Winand et al., 1991a). There was a significant 3-fold lower affinity of DM-CCK as compared to (Thr,Nle)-CCK-9 for the low-affinity binding sites (see Table I).

We next compared the stimulation of amylase secretion from rat pancreatic acini by DM-CCK and (Thr,Nle)-CCK-9 (known to be as potent as CCK-8 (Moroder et al., 1981)). The dose-response curve of DM-CCK exhibited CCK-typical up and down strokes (Figure 9). Although the lipo-CCK

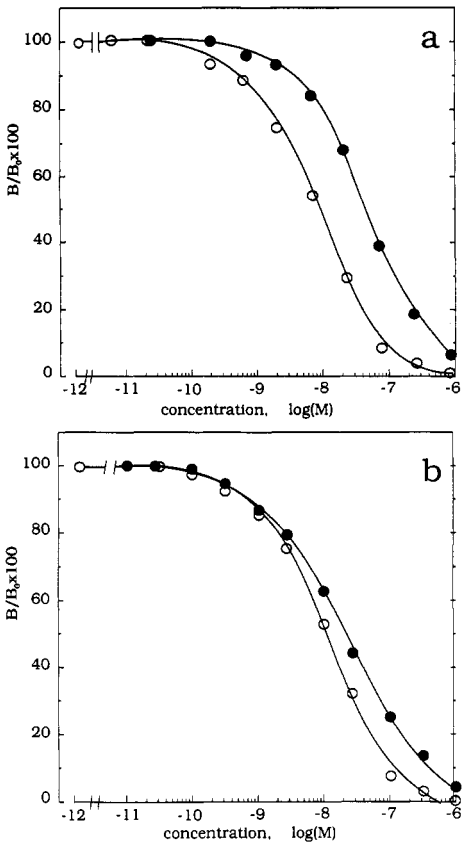

FIGURE 8: Receptor binding affinities of (Thr,Nle)-CCK-9 (○) and DM-CCK (●) after 45-min (a) and 3-h (b) incubation with isolated rat pancreatic acini using radiolabeled desaminotyrosyl-(Thr,Nle)-CCK-9 as tracer. Results are expressed as % B/B_0 where B_0 is tracer binding in the absence of unlabeled ligand. The data are averages of four experiments conducted in duplicate.

Table I: K_i Values and Proportions (%) of High- and Low-Affinity Sites for Inhibition of [^{125}I]-(Thr,Nle)-CCK-9 Binding by (Thr,Nle)-CCK-9 and DM-CCK[a]

peptide		binding sites[b] high affinity	low affinity
(Thr,Nle)-CCK-9	K_i (nM)	0.17 ± 0.08	17 ± 3
	%	42 ± 7	58 ± 7
DM-CCK	K_i (nM)	0.14 ± 0.07	49 ± 7[c]
	%	40 ± 6	60 ± 6

[a] Data, derived from Figure 8b, were analyzed with the aid of the nonlinear-least-squares curve-fitting LIGAND program (Richardson & Humrich, 1984) and expressed as mean ± SEM ($n = 4$). K_i values were corrected according to Cheng and Prusoff (1973). [b] Total binding sites were 45 ± 6 fmol/mg of protein. [c] K_i values of (Thr,Nle)-CCK-9 and DM-CCK for the low-affinity sites were significantly different ($p < 0.05$).

derivative showed the same efficacy as the parent peptide, the optimal EC_{50} concentration for amylase hypersecretion with DM-CCK was 0.23 ± 0.12 nM as compared to 2.3 ± 0.9 pM ($n = 4$) for (Thr,Nle)-CCK-9. As reported in Table II, DM-CCK also increased IP_3 formation with an EC_{50} of 6.10 ± 1.50 nM as compared to 1.64 ± 0.31 nM for (Thr,Nle)-CCK-9 ($n = 4$) and the efficacies of both ligands were again similar (data not shown).

DISCUSSION

Insertion of pentagastrin, i.e. of Boc-Gly-Trp-Met-Asp-Phe-NH_2, into phospholipid bilayers has been well assessed by microcalorimetry and fluorescence experiments, but not its orientation (Surewicz et al., 1984, 1985; Epand et al., 1988). The lipid affinity of the pentagastrin most probably derives

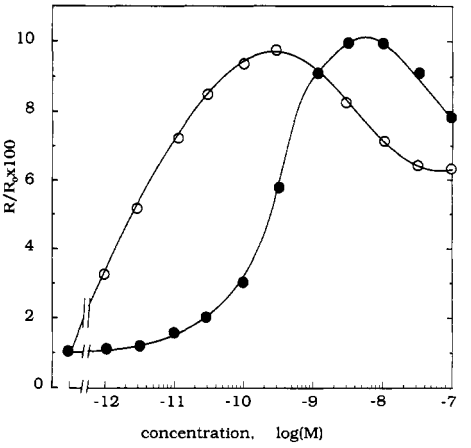

FIGURE 9: Dose-response curves of (Thr,Nle)-CCK-9 (○) and DM-CCK (●) on amylase secretion by isolated rat pancreatic acini. Results are expressed as % R/R_c where R_c is the total initial amylase content. The data are averages of four experiments conducted in duplicate.

from the hydrophobic N-terminus, since (Thr,Nle)-CCK-9, which shares the identical pentapeptide sequence, was found to interact only transiently with phospholipid SUVs, leading to their fusion and, thus, to a higher degree of order in the lipid packing, which then leads to expulsion of the disordering peptide. This interesting observation raises the question of whether a similar physical phenomenon is implicated in the known fusion of neurotransmitter vesicles with the membrane of the synaptic junctions and concomitant release of the peptide (Brown, 1991; Crawley, 1991), since CCK peptides are known to act as neurotransmitters. On the other hand, the observed expulsion of the CCK peptide from larger DMPC bilayers should not preclude interactions of CCK with natural membranes, which are known to have a bilayer packing significantly less ordered than DMPC.

By incorporation of the double-tailed lipid moiety at the N-terminus of the CCK nonapeptide, the site of anchorage in the bilayer is well defined. The NMR experiments clearly confirmed a bending of the peptide head group with insertion of the C-terminus into inner compartments as postulated from the fluorescence data (Romano et al., 1993a). MD simulations of DM-CCK in the two-phase H_2O/CCl_4 cell showed that the tryptophan-6 side chain remains in close contact with the fatty acid chains, whereby the relative position of the phenylalanine-9 and tryptophan-6 side chains as well as the backbone folding is restricted in a limited conformational space with an amphipathic array relative to the H_2O/CCl_4 interface but also with respect to the C- and the N-terminus of the peptide moiety. This is clearly illustrated by the density profiles and solvation shells of selected diagnostic atoms of the molecule.

Regarding the whole molecule, i.e. including the fatty acid chains, the chain reversal in the peptide moiety produces a conical shape, which in view of its mismatch of the cross-section areas between head group and fatty acid chains (Figure 10), if compared to those of DMPC (see Figure 10), is expected to greatly affect the order of DMPC bilayers. This would explain the relative fluidity of the DM-CCK vesicles, but also their tendency to merge into DMPC vesicles with formation of less disturbing clusters as observed in microcalorimetric experiments (Romano et al., 1993a). Independently of whether such clusters are also formed in natural membranes, an escape of the DM-CCK from membrane bilayer is energetically highly unfavored. Since the DM-CCK/membrane bilayer merging process should occur rapidly and quantitatively, as expected from the model experiments, the observed ability of DM-CCK to compete with the CCK tracer

Table II: K_i Values for Binding to Low-Affinity Sites, EC_{50} Values for IP_3 Formation and Amylase Secretion, and Amplification Factors for (Thr,Nle)-CCK-9 and DM-CCK in Rat Pancreatic Acini

peptide	K_i (nM) for low-affinity sites	EC_{50} (nM) for IP_3 (I)	EC_{50} (pM) for amylase (A)	K_i/EC_{50}(A)	K_i/EC_{50}(I)	EC_{50}(I)/ EC_{50}(A)
(Thr/Nle)-CCK-9	17 ± 3	1.64 ± 0.31	2.29 ± 0.92	7429	10	716
DM-CCK	49 ± 7[a]	6.10 ± 1.50[a]	229 ± 120[a]	214[a]	8	27[a]

[a] Values significantly different ($p < 0.05$) from those with (Thr,Nle)-CCK-9 ($n = 4$).

for the receptor binding site can only be explained by two-dimensional membrane-bound migration to the receptor. The lower association rate of the lipophilic derivative, if compared to that of the unmodified parent CCK peptide, has therefore to be attributed to the strong interdigitation of the bis(fatty acyl) moiety with the membrane lipids as well as to the large head group. This is further supported by previous findings related to similar lipogastrin derivatives where increasing the chain length of the fatty acids was found to reduce the receptor binding affinity (Romano et al., 1992). The diffusion coefficient for a lipid in a membrane equals around 5×10^{-9} cm^2/s (K. Jacobson, private communication); i.e., on average, it covers a distance of 140 μm in 1 s. In a first approximation, this value is also assumed for DM-CCK because of interdigitation of the fatty acid chains with the membrane lipids. Approximating the shape of (Thr,Nle)-CCK-9 as spherical with a radius of ca. 20 water molecules (1.4 Å each), Stokes' law $D \sim r^{-1}$ leads to a diffusion coefficient of $(1/20)(2.5 \times 10^{-5})$ $cm^2/s = 1.3 \times 10^{-6}$ cm^2/s for the CCK peptide, where 2.5×10^{-5} cm^2/s is the diffusion coefficient of pure water (Trappeniers et al., 1965). Using the corresponding Einstein relationship for three-dimensional diffusion, (Thr,Nle)-CCK-9 covers an average distance of 2700 μm in 1 s, which is an order of magnitude higher than that for two-dimensional diffusion of DM-CCK, assuming that for two (three-) dimensional diffusion the Einstein relationship between mean-square distance (msd) and diffusion coefficient (D) is valid; i.e., $msd = 4(6)Dt$. In the case of a two-dimensional diffusion of (Thr,Nle)-CCK-9 on the bilayer surface, the average distance covered by the peptide is reduced to 80% of its diffusion coefficient is assumed to be that in water.

On the other hand, the general concept of the spatial transmembrane structure of receptors with seven membrane-spanning domains raises the immediate question of how a membrane-bound peptide may bypass the bulky boundary domains resulting from the extracellular, partly carbohydrated loop structures and find its way to the binding cleft. Since an escape of the double-tailed lipopeptide into the extracellular water phase is energetically highly unfavored, a lateral penetration at the lipid/water boundary, where spectroscopic measurements and MD simulations are locating the lipopeptide in a folded form, has to take place. This would imply remarkable flexibility of the complex receptor structure, particularly in view of the large size of the structured ligand. Interestingly, its folded form exhibits a hydrophobic head in the peptide moiety consisting of the phenylalanine side chain, which may initiate the insertion of the peptide, followed by penetration of at least the peptide moiety into the binding cleft.

Intriguing remains the lower potency of DM-CCK in stimulating amylase release. CCK is generally believed to stimulate secretion of digestive enzymes from rat pancreatic acini by activating phospholipase C, which hydrolyzes the membrane lipid phophatidylinositol bis(phosphate) with release of inositol tris(phosphate) and diacylglycerol, increase of cytosolic calcium, and activation of protein kinase C (Sankaran et al., 1980; Hootman & Williams, 1987; Gardner & Jensen, 1987; Matozaki et al., 1989; Menozzi et al., 1991). These CCK actions are mediated by three classes or states of the CCK receptor which have been well characterized pharmacologically (Vinayek et al., 1993). Of these three CCK receptor states, the high- and low-affinity states are involved in the competitive binding experiments, whereas the low-affinity state mediates the upstroke of the dose response curve and the very-low-affinity state the downstroke.

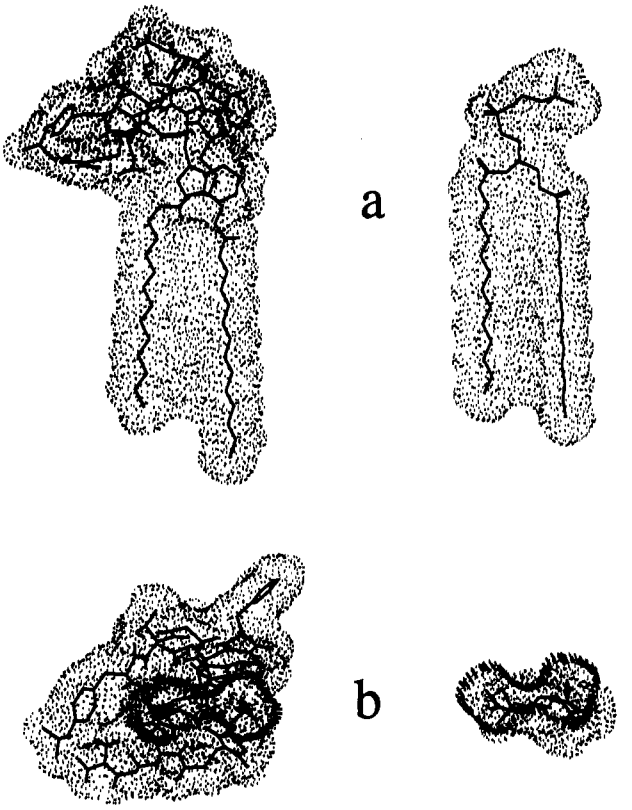

FIGURE 10: Shape comparison of Connolly surfaces of DM-CCK (left) and DMPC (right), both with extended fatty acid chains, to illustrate the mismatch of cross-section areas between head group and fatty acid chains of DM-CCK: (a) side view; (b) top view.

The biological data obtained with DM-CCK and (Thr,Nle)-CCK indicate a similar amplification factor between binding to the functional low-affinity receptors and IP_3 production for both peptides (Table II), suggesting that the coupling of Gq between receptor and phospholipase C was equivalent. However, the amplification factor between IP_3 formation and amylase secretion was 27 times lower with DM-CCK than with (Thr,Nle)-CCK-9. Therefore, the difference in amplification between IP_3 formation and the final biological response was responsible for the difference in amplification between binding and amylase secretion (a 35-fold factor between DM-CCK and (Thr,Nle)-CCK-9). Stimulus-secretion coupling in pancreatic acini involves several G-proteins (e.g. see Winand et al. 1991b). It is conceivable that DM-CCK, due to its membrane-bound state, occupies low-affinity receptors in such a way that they are poorly coupled to G-proteins distinct from Gq but contribute nevertheless to the normal response.

To conclude, the findings of the present study confirm that a membrane-bound pathway in the mechanism of hormone receptor binding processes is indeed possible and that the preorientation and prefolding of the ligand in the lipid bilayer could play a decisive role not only in the binding event but also in the lateral penetration of the complex transmembrane receptor molecule.

REFERENCES

Bax, A., Sklenar, V., Clore, G. M., & Gronenborn, A. M. (1987) *J. Am. Chem. Soc. 109*, 6511–6513.

Berendsen, H. J. C., Postma, J. P. M., van Gunsteren, W. F., & Hermans, J. (1981) in *Intermolecular Forces* (Pullman, B., Ed.), Reidel, Dordrecht, The Netherlands.

Bodenhausen, G., Vold, R. L., & Vold, R. R. (1980) *J. Magn. Reson. 37*, 92–106.

Brown, A. G. (1991) in *Nerve Cells and Nervous Systems. An Introduction to Neuroscience* (Brown, A. G., Ed.) pp 61–71, Springer Verlag, London.

Cheng, Y., & Prusoff, W. H. (1973) *Biochem. Pharmacol. 22*, 3099–3108.

Crawley, J. N. (1991) *Trends Pharmacol. Sci. 12*, 232–236.

Dehaye, J. P., Winand, J., Damien, C., Gomez, F., Poloczek, P., Robberecht, P., Vandermeers, A., Vandermeers-Piret, M.-C., Stiévenart, M., & Christophe, J. (1986) *Am. J. Physiol. 251*, G602–G610.

Dixon, R. A., Sigal, I. S., Candelore, M. R., Register, R. B., Rands, E., & Strader, C. D. (1987) *EMBO J. 6*, 3269–3275.

Dockray, G. J. R. (1976) *Nature (London) 264*, 568–572.

Driscoll, P. C., Clore, G. M., Beress, L., & Gronenborn, A. M. (1989) *Biochemistry 28*, 2178–2187.

Epand, R. M., Surewicz, W. K., & Yeagle, P. (1988) *Chem. Phys. Lipids 49*, 105–110.

Gaisano, H. Y., & Miller, L. J. (1992) *Biochem. Biophys. Res. Commun. 187*, 498–506.

Gardner, J. D., & Jensen, R. T. (1987) in *Physiology of the Gastrointestinal Tract* (Johnson, L. R., Ed.) 2nd ed., pp 1109–1127, Raven Press, New York.

Hicks, R. P., Beard, D. J., & Yonng, J. K. (1992) *Biopolymers 32*, 85–96.

Hootman, S. R., & Williams, J. A. (1987) in *Physiology of the Gastrointestinal Tract* (Johnson, L. R., Ed.) 2nd ed., pp 1129–1146, Raven Press, New York.

Hulme, E. C., Birdsall, N. J., & Bucköey, N. J. (1990) *Annu. Rev. Pharmacol. Toxicol. 30*, 633–673.

Karnik, S. S., Sakmann, J. P., Chen, H. A., & Khorana, G. (1988) *Proc. Natl. Acad. Sci. U.S.A. 85*, 8459–8463.

Kopin, A. S., Lee, Y.-M., McBride, E. W., Miller, L. J., Lu, M., Lin, H. Y., Kolakowski, L. F., & Beinborn, M. (1992) *Proc. Natl. Acad. Sci. U.S.A. 89*, 3603–3609.

Marion, D., & Wüthrich, K. (1983) *Biochem. Biophys. Res. Commun. 113*, 967–974.

Matozaki, T., & Williams, J. A. (1989) *J. Biol. Chem. 264*, 14729–14734.

Menozzi, D., Vinayek, R., Jensen, R. T., & Gardner, J. D. (1991) *J. Biol. Chem. 266*, 10385–10391.

Moroder, L., Musiol, H. J., & Siglmüller, G. (1990) *Synthesis* 889–892.

Moroder, L., Romano, R., Weyher, E., Svoboda, M., & Christophe, J. (1993a) *Z. Naturforsch. 48b*, 1419–1430.

Moroder, L., D'Ursi, A., Picone, D., Amdoleo, P. & Temussi, P. A. (1993b) *Biochem. Biophys. Res. Commun. 190*, 741–746.

Moroder, L., Göhring, W., Nyfeler, R., Scharf, R., Thamm, P., & Wendlberger, G. (1983) *Hoppe-Seyler's Z, Physiol. Chem. 364*, 151–171.

Moroder, L., Wilschowitz, L., Gemeiner, M., Göhring, W., Knof, S., Scharf, R., Thamm, P., Gardner, J. D., Solomon, T. E., & Wünsch, E. (1981) *Hoppe-Seyler's Z. Physiol. Chem. 362*, 929–942.

Müller, L. (1987) *J. Magn. Reson. 72*, 191–196.

Mutt, V., & Jorpes, J. E. (1968) *Eur. J. Biochem. 6*, 156–162.

Plateau, P., & Gueron, M. (1982) *J. Am. Chem. Soc. 104*, 7311–7312.

Rebertus, D. W., Berne, B. J., & Chandler, D. J. (1979) *Chem. Phys. 70*, 3395–3400.

Rehfeld, J. F., Hansen, H. F., Marley, P. D., & Stengard-Petersen, K. (1985) *Ann. N.Y. Acad. Sci. 448*, 11–23.

Richardson, A., & Humrich, A. L. (1984) *Trends Pharmacol. Sci. 5*, 47–49.

Robberecht, P., Deschodt-Lanckman, M., & Vanderhaeghen, J. J. (1978) *Proc. Natl. Acad. Sci. U.S.A. 75*, 524–526.

Romano, R., Bayerl, T. M., & Moroder, L. (1993a) *Biochim. Biophys. Acta 1151*, 111–119.

Romano, R., Musiol, H.-J., Weyher, E., Dufresne, M., & Moroder, L. (1992) *Biopolymers 32*, 1545, 1558.

Romano, R., Dufresne, M., Prost, M.-C., Bali, J.-P., Bayerl, T. M., & Moroder, L. (1993b) *Biochim. Biophys. Acta 1145*, 235–242.

Sakamoto, C., Williams, J. A., & Goldfine, I. D. (1984) *Biochem. Biophys. Res. Commun. 124*, 497–502.

Sankaran, H., Goldfine, I. D., Deveney, C. W., Wong, K.-Y., & Williams, J. A. (1980) *J. Biol. Chem. 255*, 1849–1853.

Savarese, T. M., & Fraser, C. M. (1992) *Biochem. J. 283*, 1–19.

Schwyzer, R. (1986) in *Natural Products and Biological Activities* (Imura, H., Goto, T., Murachi, T., & Nakajima, T., Eds.) pp 197–207, Tokyo Press, Elsevier, Tokyo.

Schwyzer, R. (1991) *Biopolymers 31*, 785–792.

Sklenar, V., & Bax, A. (1987) *J. Magn. Reson. 74*, 469–479.

Surewicz, W. K., & Epand, R. M. (1984) *Biochemistry 23*, 6072–6077.

Svoboda, M., Lambert, M., Moroder, L., & Christophe, J. (1984) *J. Chromatogr. 296*, 199–211.

Trappeniers, N. J., Gerritsma, C. J., & Oosting, P. H. (1965) *Phys. Lett. 18*, 256–257.

Vinayek, R., Patto, R. J., Menozzi, D., Gregory, J., Mrozinski, J. E., Jensen, R. T., & Gardner, J. D. (1993) *Biochim. Biophys. Acta 1176*, 183–191.

Wank, S. A., Jensen, R. T., & Gardner, J. D. (1988) *Am. J. Physiol. 255*, G106–G112.

Wank, S. A., Pisegna, J. R., & De Weerth, A. (1992a) *Proc. Natl. Acad. Sci. U.S.A. 89*, 8691–8693.

Wank, S. A., Harkins, R., Jensen, R. T., Shapira, H., De Weerth, A., & Slattery, T. (1992b) *Proc. Natl. Acad. Sci. U.S.A. 89*, 3123–3129.

Winand, J., Poloczek, P., Delporte, C., Moroder, L., Svoboda, M., & Christophe, J. (1991a) *Biochim. Biophys. Acta 1080*, 181–190.

Winand, J., Delporte, C., Poloczek, P., Cantraine, F., Dehaye, J.-P., Christophe, J. (1991b) *Second Messengers Phosphoproteins 13*, 173–186.